Hydrogen sulfide inhibits mitochondrial fission in neuroblastoma N2a cells through the Drp1/ERK1/2 signaling pathway

PEIFENG QIAO, FENGLI ZHAO, MENGJIE LIU, DAN GAO, HUA ZHANG and YONG YAN

Department of Neurology, The First Affiliated Hospital of Chongqing Medical University, Chongqing 400016, P.R. China

Abstract. Hydrogen sulfide (H_2S) has been demonstrated to have various effects on mitochondrial function. The aim of the present study was to investigate the effects of H_2S on mitochondrial fission and the potential underlying mechanisms of these effects. Transmission electron microscopy analysis demonstrated that sodium hydrosulfide (NaHS, a donor of H_2S) inhibited mitochondrial fission in a dose- and time-dependent manner. Treating neuro-2a (N2a) mouse neuroblastoma cells with 400 μM NaHS for 16 h significantly increased the % of elongated mitochondria and reduced the number of mitochondria per cell compared with untreated cells. In addition, the viability and ATP generation of N2a cells that were treated with various concentrations of NaHS was examined. The results demonstrated that treatment with 400 and 600 μM NaHS increased cell viability and ATP generation compared with untreated cells. To further understand the effects of H_2S on mitochondrial morphology, the protein and mRNA expression levels of dynamin 1 like (Dnm1l, also known as Drp1) were examined, and the results demonstrated that NaHS dose-dependently reduced Drp1 mRNA and protein levels, consistent with the mitochondrial morphology changes. To determine whether H_2S affects mitochondrial morphology through Drp1 expression, Drp1 was overexpressed in N2a cells using a lentivirus encoding the Drp1 cDNA. It was observed that Drp1 overexpression reversed the effects of NaHS. Furthermore, NaHS promoted the phosphorylation of extracellular signal-regulated kinase (ERK) 1/2, and the effects of NaHS on Drp1 expression were abolished by an ERK1/2 inhibitor (PD98059). The results of the present study indicate that the H_2S-induced decrease in Drp1 mRNA and protein levels and mitochondrial fission may involve the ERK1/2 signaling pathway. The present study suggests that H_2S may be used in the future as a potential therapeutic for diseases that may be mediated by abnormal mitochondria fragmentation, such as Alzheimer's disease.

Introduction

Mitochondria are cytoplasmic organelles that are responsible for most of the energy supply of cells. Furthermore, they are important in regulating various cellular processes, including calcium homeostasis, signaling pathways, apoptosis and the production of reactive oxygen species (ROS) (1). Within cells, mitochondria are highly dynamic organelles, transitioning from a giant tubular network to small round organelles through reversible fission and fusion (2). These opposing processes work in concert to maintain the shape, size and number of mitochondria, as well as their physiological function. Alterations in mitochondrial dynamics have an effect on the majority of aspects of mitochondrial function, including the stability of mitochondrial DNA, respiratory capacity, apoptosis, responses to cellular stress and mitophagy (3-7). Mitochondrial dynamics are regulated by mitochondrial dynamics-related GTPase proteins. Dynamin 1 like (Dnm1l, also known as Drp1) is one of the GTPase proteins that promotes mitochondrial fragmentation, whereas the expression of a dominant-negative form of Drp1 inhibits mitochondrial fission and thereby apoptosis (8). Other studies have demonstrated that the inhibition of mitochondrial fission protects against neurotoxicity (9,10) and neurodegeneration in the cerebellum (11). In addition, numerous reports have indicated that excessive mitochondrial fission contributes to Alzheimer's disease (AD) pathogenesis via synaptic damage and neuronal death (12,13). Therefore, the protection of mitochondria from fragmentation may provide a novel therapeutic target for neurodegenerative disorders, such as AD (14,15).

Hydrogen sulfide (H_2S) has been identified as a biological gaseous transmitter alongside nitric oxide and carbon monoxide (16). In mammals, H_2S is endogenously produced by cystathionine-β-synthase, cystathionine-γ-lyase and 3-mercaptopyruvate sulfurtransferase, with L-cysteine as the dominant substrate (17,18). H_2S is recognized as a biological mediator that serves various functions, including neuromodulation, the regulation of vascular tone, cytoprotection, anti-inflammation, oxygen sensing and angiogenesis, in addition to mitochondrial functions (19-22). A number of

Correspondence to: Dr Peifeng Qiao or Dr Yong Yan, Department of Neurology, The First Affiliated Hospital of Chongqing Medical University, 1 Youyi Road, Chongqing 400016, P.R. China
E-mail: 382467434@qq.com
E-mail: yyanpro@126.com

recent studies focused on the effects of H$_2$S on mitochondrial function. H$_2$S has been demonstrated to suppress mitochondrial ROS production, increase ATP production and improve the loss of mitochondrial membrane potential under stress conditions (23). However, since mitochondrial dynamics are important for essential mitochondrial functions, and since mitochondrial fission is abnormally increased in affected neurons in neurodegenerative diseases, inhibitors of mitochondrial fission may be promising therapeutic targets for the treatment of neurodegenerative diseases (24). Therefore, the present study focused on the effects of H$_2$S on mitochondrial fission and fusion and the potential underlying mechanisms.

Materials and methods

Materials. Sodium hydrosulfide (NaHS), an H$_2$S donor, was obtained from Sigma-Aldrich (Merck KGaA, Darmstadt, Germany) and dissolved in sterile water. PD98059, an extracellular signal-regulated kinase (ERK) 1/2 signal pathway inhibitor, was purchased from Abcam (Cambridge, UK) and dissolved in sterile water.

Cell culture and lentiviral transduction. Neuro-2a (N2a) mouse neuroblastoma cells were purchased from the Cell Bank of Type Culture Collection of Chinese Academy of Sciences (Shanghai, China). The cells were cultured in Dulbecco's modified Eagle's medium (Invitrogen; Thermo Fisher Scientific, Inc., Waltham, MA, USA) containing 10% heat-inactivated fetal bovine serum (Gibco; Thermo Fisher Scientific, Inc.) and 1% penicillin and streptomycin, and were maintained at 37°C with 95% humidified air and 5% CO$_2$. The cells (2×10^5) were plated in 35 mm dishes and incubated for 48 h. On the third day, the medium was removed and the cells were washed with PBS. Subsequently, the cells were exposed to serum-free culture medium for 24 h. The experimental treatments were also performed in serum-free culture medium. Ready-to-use lentiviral particles for a Drp1-overexpressing lentiviral vector (LV-Drp1) and a control vector (LV-empty) were purchased from GeneChem Co., Ltd. (Shanghai, China; cat. nos. V20140402006 and V20140402007 respectively). The LV-Drp1 and the LV-empty virus-containing media were added to the N2a cells with a multiplicity of infection (MOI) of 5. Non-transduced cells were used as controls. To calculate the amount of virus required for a certain MOI, the following formula was used: Total ml of virus required=number of cells xdesired MOI/(plaque forming units/ml). All of the media was changed 12 h post-transduction. Three days after transduction, western blot analysis was performed to evaluate transduction efficiency.

Transmission electron microscopy. To determine whether mitochondrial morphology was altered in the N2a cells, transmission electron microscopy was performed. The N2a cells were prefixed in a 2.5% glutaraldehyde solution overnight at 4°C and post-fixed in cold 1% aqueous osmium tetroxide for 1 h at 4°C. The samples were rinsed three times with PBS, dehydrated in a graded series of 25-100% ethanol, embedded in fresh resin and polymerized at 60°C for 24 h. The samples were sectioned on a Leica EM UC6 ultramicrotome at 60-80 nm and collected on pioloform-coated Cu2*1 oval slot grids (Electron Microscopy Sciences, Hatfield, PA, USA). The

sections were subsequently examined under a Hitachi-7500 transmission electron microscope (Hitachi, Ltd., Tokyo, Japan). The number of mitochondria per cell was counted in ≥10 cells in each group. The proportion of 'elongated' mitochondria was estimated as the number of mitochondria with a length that was at least twice the width, divided by the total number of mitochondria counted (25).

Determination of cell viability. Cell viability was assessed by the reduction of MTT. Briefly, 20 µl MTT (5 mg/ml; Sigma-Aldrich; Merck KGaA) was added to each well and the cells were incubated at 37°C for 1 h. The cells were washed with PBS and the formazan dye was dissolved in dimethyl sulfoxide. The amount of converted formazan dye was measured at 570 nm on a PowerWave reader (Biotek Instruments, Inc., Winooski, VT, USA). This method detects complex II-dependent mitochondrial activity and is often used to estimate mitochondrial function and/or cell viability.

Measurement of ATP levels. ATP levels were determined using an ATP Bioluminescence Assay kit CLS II (Sigma-Aldrich; Merck KGaA) following the manufacturer's instructions (26). Briefly, cells were harvested using the provided lysis buffer, incubated on ice for 15 min and centrifuged at 13,000 x g for 10 min at 4°C. ATP levels were measured using a luminescence plate reader (Molecular Devices, LLC, Sunnyvale, CA, USA) with an integration time of 10 sec.

Reverse transcription-quantitative polymerase chain reaction (RT-qPCR) analysis. Total RNA was extracted from the cells using TRIzol reagent (Takara Biotechnology Co., Ltd., Dalian, China) according to the manufacturer's protocol. After evaluating the concentration of total RNA by a UV spectrophotometer, total RNA was reverse-transcribed using the PrimeScript RT reagent kit (Takara Biotechnology Co., Ltd.). qPCR was performed using SYBR Premix Ex Taq II (Takara Biotechnology Co., Ltd.) and a CFX96 Real-Time PCR Detection System (Bio-Rad Laboratories, Inc., Hercules, CA, USA). mRNA expression was normalized to β-actin and relative expression was calculated using the 2(-Delta Delta C(q)) method (27). The primer sequences (Sangon Biotech Co., Ltd., Shanghai, China) were as follows: Drp1, forward 5'-GGC ATTACAAGGAGCCAGTC and reverse 5'-CAGCAGGTT CAAGTCAGCAA; β-actin, forward 5'-CACCCGCGAGTA CAACCTTC and reverse 5'-CCCATACCCACCATCACACC. Each experiment was performed in triplicate.

Western blot assay. Cells were harvested by scraping and centrifugation at 220 x g at room temperature for 5 min, washed twice with ice-cold PBS and re-suspended in lysis buffer (50 mM Tris, 150 mM NaCl, 1% NP-40, 0.1% SDS, 10 mM EDTA, 1 mM PMSF and 0.5% sodium deoxycholate), according to the manufacturer's protocol (KeyGEN Biotech Co., Ltd., Nanjing, China). Soluble proteins were collected by centrifugation at 12,000 x g for 15 min at 4°C. Protein concentrations were determined using the bicinchoninic acid method. Protein (30 µg) was separated by 10% SDS-PAGE and subsequently transferred onto polyvinylidene difluoride membranes. After the membranes were blocked with 5%

skim milk for 1 h at room temperature, they were incubated with antibodies against Drp1 (1:1,000; cat. no. ab56788; Abcam, Cambridge), phosphorylated-(p)-ERK1/2 (1:1,000, cat. no. sc-81492; Santa Cruz Biotechnology, Inc., Dallas, TX, USA), total (t)-ERK1/2 (1:1,000, cat. no. sc-514302; Santa Cruz Biotechnology, Inc.) and β-actin (1:1,000, cat. no. sc-130301; Santa Cruz Biotechnology, Inc.) overnight at 4°C. Subsequently, the membranes were incubated with a secondary horseradish peroxidase-conjugated antibody (1:2,000; cat. no. A0216; Beyotime Instistute of Biotechnology, Shanghai, China) for 2 h at room temperature and the SuperSignal West Pico Chemiluminescent Substrate (Thermo Fisher Scientific, Inc.) was used for detection. Densitometric quantification of blots was performed using Alphapart11 Ease version 5.0 (ProteinSimple; Bio-Techne, Minneapolis, MS, USA) and expression levels were calculated as a ratio relative to the control level.

Statistical analysis. All data are expressed as the mean + standard error of the mean. Differences between groups were analyzed by ANOVA followed by the Student-Newman-Keuls test. All statistical analyses were performed using SPSS version 17.0 (SPSS, Inc., Chicago, IL, USA). $P<0.05$ was considered to indicate a statistically significant difference.

Results

The effect of NaHS treatment on mitochondrial fission. The present study used transmission electron microscopy to determine changes in the number and morphology of mitochondria in the cell bodies of N2a cells. Control untreated and NaHS-treated N2a cells were collected for transmission electron microscopy imaging (Fig. 1). In the present study, NaHS was used as a donor for H_2S, since it readily releases H_2S upon its suspension in water. Initially, the cells were treated with different concentrations of NaHS for 16 h (Fig. 1A-C). A dose-dependent increase in the % of elongated mitochondria was observed following NaHS treatment compared with control (Fig. 1B; control, 38.75±2.39%; NaHS 100 µM, 48.50±3.01%; NaHS 200 µM, 61.75±1.97%; NaHS 400 µM, 68.75±2.39%). By contrast, the number of mitochondria per cell was decreased in a dose-dependent manner following NaHS treatment compared with control (Fig. 1C; control, 39.25±3.25; NaHS 100 µM, 32.75±1.10, NaHS 200 µM, 25.5±1.32; NaHS 400 µM, 21.25±1.31). Next, cells were treated with 400 µM NaHS for different durations (Fig. 1D-F). Treatment with 400 µM NaHS for 8 and 16 h resulted in an increased % of elongated mitochondria (Fig. 1E; control, 42.50±2.15%; 8 h, 52.75±2.35%; 16 h, 63.75±1.75%) and a reduced number of mitochondria per cell (Fig. 1F; control, 32.75±1.25; 8 h, 22.50±1.89; 16 h, 18.75±1.25), compared with control. The differences between the control group and the 400 µM NaHS groups at 8 and 16 h were statistically significant ($P<0.01$). These results indicate that NaHS treatment may inhibit mitochondrial fission in a dose- and time-dependent manner.

The effect of NaHS treatment on cell viability and mitochondrial ATP synthesis. The MTT assay was used to evaluate the effect of H_2S on cell viability. As demonstrated in Fig. 2A, NaHS treatment for 16 h increased cell viability

in a dose-dependent manner (control, 0.97±0.01; NaHS 100 µM, 1.03±0.04; NaHS 200 µM, 1.13±0.04; NaHS 400 µM, 1.24±0.02; NaHS 600 µM, 1.33±0.03) compared with control. In addition, the rate of ATP production was gradually increased following NaHS treatment for 16 h, compared with control (Fig. 2B; control, 0.97±0.02; NaHS 100 µM, 1.03±0.04; NaHS 200 µM, 1.10±0.04; NaHS 400 µM, 1.24±0.02; NaHS 600 µM, 1.34±0.02). These results indicated that H_2S increased cell viability and mitochondrial function in a dose-dependent manner.

NaHS reduces the mRNA and protein expression of Drp1. To further understand the effects of H_2S on mitochondrial morphology changes, the protein and mRNA expression levels of Drp1, an important regulator of mitochondrial fission, were examined. Using RT-qPCR and western blotting, the results demonstrated that treatment with NaHS (200 and 400 µM) for 16 h significantly decreased Drp1 mRNA and protein expression levels compared with control (Fig. 3), consistent with the reduction of mitochondrial fission observed in NaHS-treated N2a cells (Fig. 1). These results indicate that H_2S may inhibit mitochondrial fission by inhibiting Drp1 mRNA and protein expression.

Overexpression of Drp1 reverses the mitochondrial morphology changes induced by H_2S. To determine whether H_2S affects mitochondrial morphology by affecting Drp1 expression, Drp1 was overexpressed in N2a cells using a lentivirus encoding Drp1 cDNA (LV-Drp1). Western blotting confirmed that the cells in the LV-Drp1 group stably overexpressed Drp1 compared with the control group and the empty vector group (LV-empty; Fig. 4A and B). Transmission electron microscopy demonstrated that NaHS treatment for 16 h inhibited mitochondrial fission and that this inhibition was reversed by NaHS and LV-Drp1 co-treatment (Fig. 4C). In the NaHS-treated group, mitochondrial fission was significantly inhibited compared with the control group; the % of elongated mitochondria was increased (control, 38.75±1.49%; NaHS 400 µM, 60.50±2.10%), and the number of mitochondria per cells was decreased (control, 32.75±1.25; NaHS 400 µM, 18.25±1.70). However, this effect was reversed by LV-Drp1 trasduction. Compared with the NaHS-treated group, the NaHS and LV-Drp1 co-treated group displayed significantly fewer elongated mitochondria (NaHS 400 µM, 60.50±2.10%; NaHS 400 µM + LV-Drp1, 37.50±1.04%) and higher number of mitochondria per cell (NaHS 400 µM, 18.25±1.70; NaHS 400 µM + LV-Drp1, 24.00±2.34). These results provide further evidence that H_2S may inhibit mitochondrial fission by inhibiting Drp1 expression.

The ERK1/2 signaling pathway is involved in the NaHS-induced decrease in Drp1 expression. To further understand the molecular mechanisms of the H_2S-induced reduction of mitochondrial fission and Drp1 expression, lysates were obtained from cells that were treated with 400 µM NaHS for 16 h and subjected to western blot analysis for p-ERK1/2 and t-ERK1/2. Treatment with 400 µM NaHS significantly increased the phosphorylation of ERK1/2 compared with untreated cells (Fig. 5A). The cells were then preincubated with PD98059 (50 µM) for 30 min before they were treated
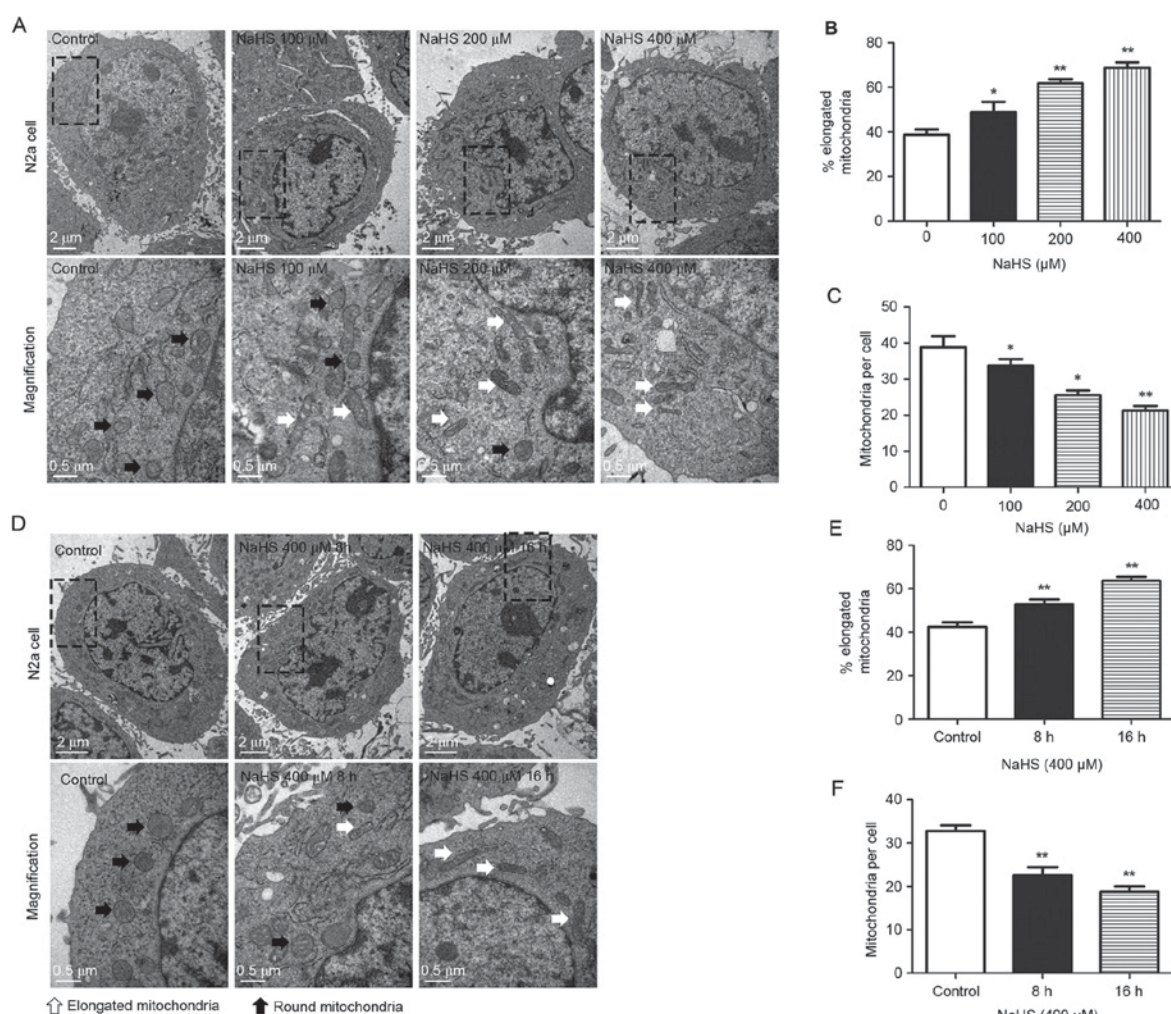
Figure 1. Transmission electron microscopy analysis of mitochondria within the cell body demonstrates an increased number of elongated mitochondria in the NaHS-treated cells. (A) Representative images of the cell bodies are presented for N2a cells treated with 0, 100, 200 and 400 μM NaHS for 16 h. Images on the bottom row are magnified images of the boxed areas in the top row. (B) Percentage of elongated mitochondria and (C) number of mitochondria per cell were calculated for N2a cells treated with 0, 100, 200 and 400 μM NaHS. (D) Representative images of the cell bodies are presented for N2a cells treated with 400 μM NaHS for 8 and 16 h, and control cells. Images on the bottom row are magnified images of the boxed areas in the top row. (E) Percentage of elongated mitochondria and (F) number of mitochondria per cell were calculated for N2a cells treated with 400 μM NaHS for 8 and 16 h, and control cells. White arrows, elongated mitochondria; black arrows, round mitochondria. Data are presented as the mean + standard error of the mean of three independent experiments (n$\geq$10 images per group). *P<0.05 and **P<0.01 vs. control. NaHS, sodium hydrosulfide; N2a, neuro-2a.
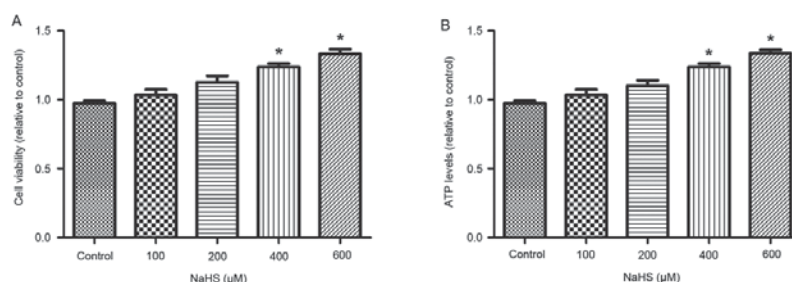

Figure 2. NaHS increases cell viability and mitochondrial ATP synthesis in a dose-dependent manner. N2a cells were treated with 100, 200, 400 and 600 μM NaHS for 16 h. (A) Viability of N2a cells subjected to various concentrations of NaHS. (B) Mitochondrial ATP synthesis in N2a cells subjected to various concentrations of NaHS. Data are presented as the mean + standard error of the mean of three independent experiments. *P<0.05 vs. control group. NaHS, sodium hydrosulfide; N2a, neuro-2a.

with 400 μM NaHS for 16 h. As presented in Fig. 5A, the NaHS-induced increase in ERK1/2 phosphorylation was reversed by PD98059 pretreatment. The effect of PD98059 on the NaHS-induced changes in Drp1 protein expression were similar to its effect on ERK1/2 phosphorylation. Pretreatment with PD98059 (50 μM) reversed the NaHS-mediated Drp1 downregulation by ~45% compared with NaHS treatment alone (Fig. 5B). These findings indicate that the ERK1/2
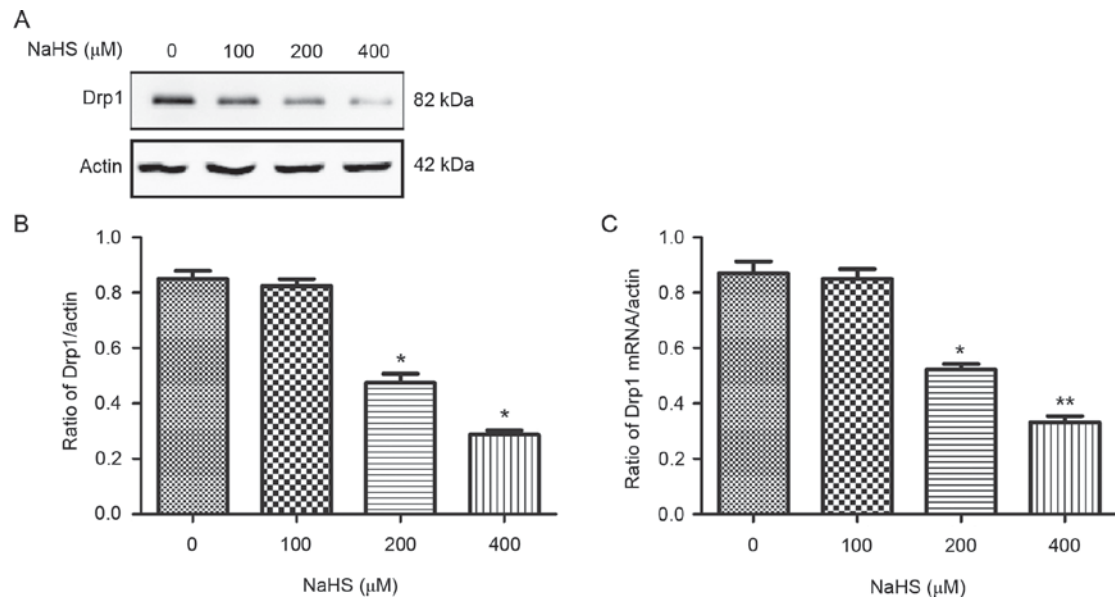
Figure 3. Effects of hydrogen sulfide on Drp1 mRNA and protein levels. N2a cells were treated with 0, 100, 200 and 400 μM NaHS for 16 h. (A) Representative western blot presenting the Drp1 and β-actin protein bands. (B) Densitometric analysis of western blots relative to β-actin expression. (C) Reverse transcription-quantitative polymerase chain reaction was performed to quantify the relative mRNA expression of Drp1. Data are presented as the mean + standard error of the mean of three independent experiments. *P<0.05 and **P<0.01 vs. the control group. Drp1, dynamin 1 like; N2a, neuro-2a; NaHS, NaHS, sodium hydrosulfide.
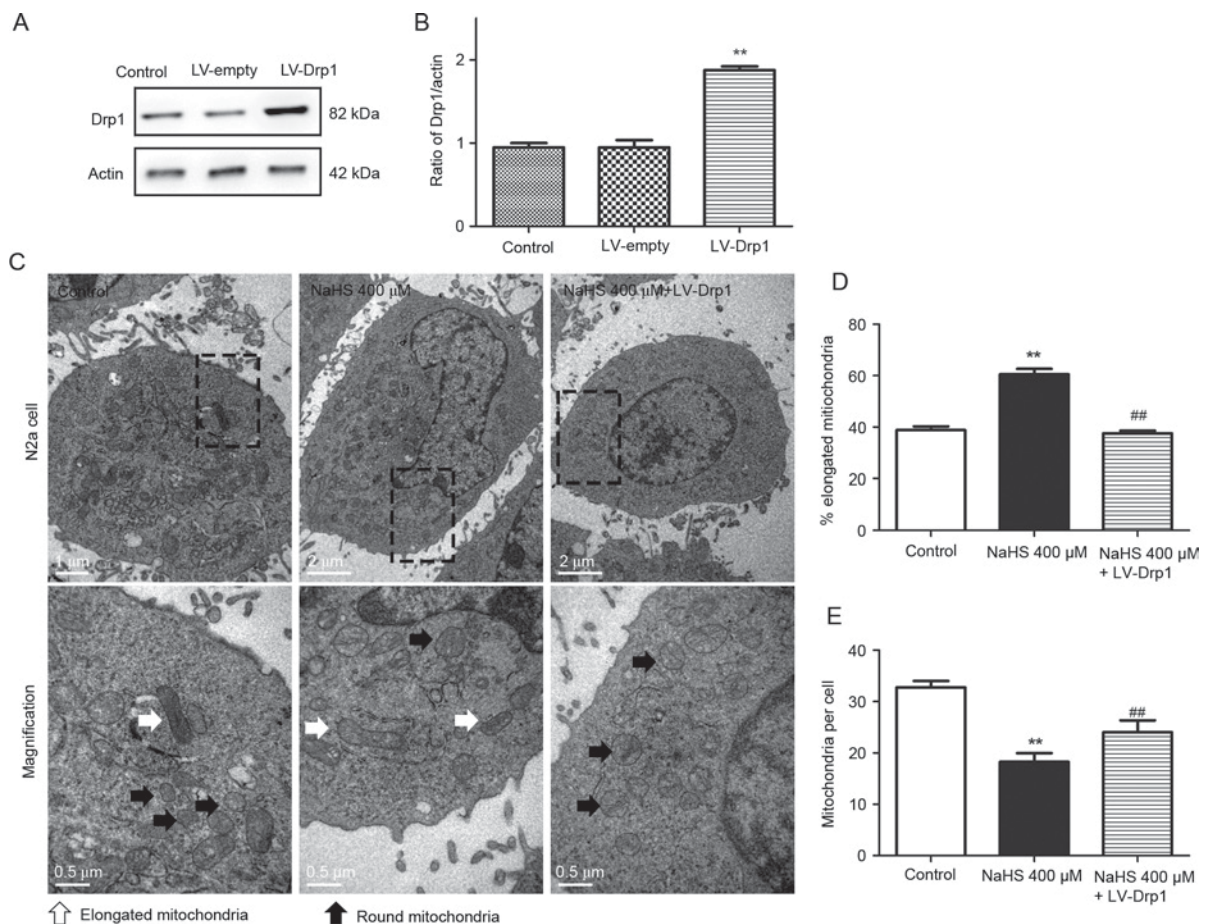

Figure 4. Overexpression of Drp1 reverses the mitochondrial morphology changes induced by hydrogen sulfide. (A) Drp1 protein expression levels were analyzed by western blotting. (B) Densitometric analysis of western blots relative to β-actin expression. (C) Representative images of the cell bodies of N2a cells treated with 400 μM NaHS and 400 μM NaHS + LV-Drp1 for 16 h. Images on the bottom row are magnified images of the boxed areas in the top row. White arrows, elongated mitochondria; black arrows, round mitochondria. (D) Percentage of elongated mitochondria in each group. (E) Number of mitochondria per cell body in each group. n≥10 images per group. Data are presented as the mean + standard error of the mean of three independent experiments. **P<0.01 vs. the control group and $^{##}$P<0.01 vs. the 400 μM NaHS group. Drp1, dynamin 1 like; N2a, neuro-2a; NaHS, sodium hydrosulfide; LV, lentivirus; LV-Drp1, LV encoding Drp1.
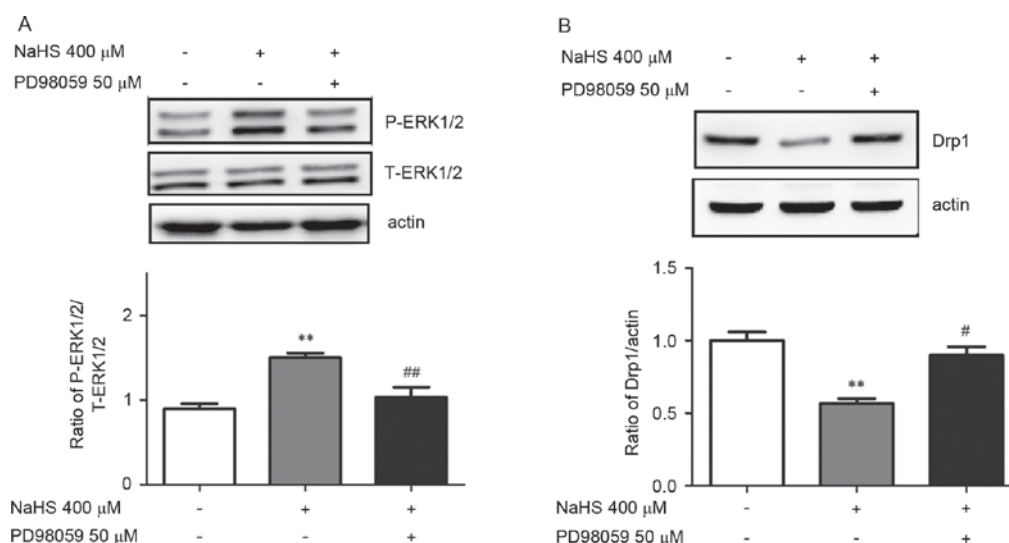
Figure 5. Activation of ERK1/2 is responsible for the hydrogen sulfide-induced decrease in Drp1 expression. (A) Western blotting and densitometric analysis demonstrated that phosphorylation of ERK1/2 was increased in cells treated with 400 μM NaHS and that this induction was blocked by PD98059. (B) Western blotting and densitometric analysis demonstrated that the effects of NaHS on Drp1 protein levels were reversed by PD98059. Densitometric analysis of western blots is presented relative to the ratios in the control untreated cells. N2a cells were treated with 400 μM NaHS for 16 h and the inhibitor was added 30 min prior to NaHS treatment. Data are presented as the mean + standard error of the mean of three independent experiments. **P<0.01 vs. the control group; #P<0.05 and ##P<0.01 vs. the 400 μM NaHS group. ERK, extracellular signal-regulated kinase; Drp1, dynamin 1 like; NaHS, sodium hydrosulfide; P, phosphorylated, T, total.

signaling pathway may be involved in the NaHS-induced decrease in mitochondrial fission and Drp1 expression.

Discussion

H$_2$S has been identified as the third gasotransmitter, and various functions of H$_2$S have been demonstrated. H$_2$S facilitates the induction of hippocampal long-term potentiation (28), modulates inflammation by suppressing leukocyte adherence and infiltration and edema formation (29), and suppresses the release of insulin by stimulating ATP-sensitive K$^+$ channels (30). Progress has also been made towards understanding the effects of H$_2$S on mitochondrial function. H$_2$S stimulates mitochondrial respiration, suppresses mitochondrial ROS production and increases ATP production (20). However, there have been no reports regarding the effects of H$_2$S on mitochondrial dynamics, which provide the foundation for the maintenance of normal mitochondrial functioning.

To the best of our knowledge, the present study is the first to demonstrate that H$_2$S inhibits mitochondrial fission. The current study used transmission electron microscopy, which is the most accurate method of detecting changes in mitochondrial morphology. To ensure the validity of the results, previously described methods were used to analyze the number of mitochondria as well as changes in their shape (25,31). The results confirmed that H$_2$S inhibited mitochondrial fission in a dose- and time-dependent manner. In addition, the present study evaluated the effect of NaHS on cell viability and ATP generation and demonstrated that 400-600 μM NaHS increased cell viability and ATP generation, indicating that NaHS may enhance mitochondrial function. This finding was consistent with previous studies (32,33). Subsequently, it was investigated whether H$_2$S may also affect the expression of Drp1, thereby affecting mitochondrial dynamics. To test this hypothesis, RT-qPCR and western blotting were performed to detect the

mRNA and protein levels of Drp1 in N2a cells following treatment with 400 μM NaHS. The results demonstrated that H$_2$S significantly affected the mRNA and protein expression levels of Drp1. Drp1 mRNA and protein expression in the cells in the 400 μM NaHS-treated group were 60% lower compared with control levels. Based on this result, we hypothesized that the impact of H$_2$S on mitochondrial morphology changes may be achieved through reduced Drp1 expression. In a previous study, Barsoum *et al* (34) observed that Drp1 overexpression leads to mitochondrial fragmentation and that dominant-negative Drp1 inhibits mitochondrial fission in primary neurons. The current study also demonstrated that Drp1 overexpression reversed the NaHS-induced inhibition of mitochondrial fission. This finding further supports our hypothesis that H$_2$S affects mitochondrial fission by reducing Drp1 expression.

To further elucidate the molecular mechanisms of the effects of H$_2$S on Drp1 expression and mitochondrial fission, the ERK1/2 pathway was analyzed. In a previous study, Zhang *et al* (35) demonstrated that H$_2$S increases ERK1/2 phosphorylation, and downregulates β-site amyloid precursor protein cleaving enzyme 1 expression and amyloid β1-42 release in PC12 cells. Gan *et al* (36) also reported that inhibiting ERK1/2 activation attenuates aberrant mitochondrial morphology and function in AD hybrid cells. The results of these studies indicate that there may be a specific association between H$_2$S, ERK1/2 activation and changes in mitochondrial morphology. To investigate this, the present study measured ERK1/2 phosphorylation in N2a cells following treatment with NaHS and the ERK1/2 signaling pathway inhibitor PD98059. The results demonstrated that H$_2$S increased ERK1/2 phosphorylation and that PD98059 blocked this effect, indicating that H$_2$S does affect ERK1/2 activation. In addition, the present study investigated whether PD98059 affects H$_2$S-induced mitochondrial fission and observed that PD98059 partially suppressed the effect of H$_2$S on mitochondrial fission. These results indicate that the ERK1/2 signaling pathway

may be crucial for the H$_2$S-induced decrease in mitochondrial fission. The effects of inhibitor pretreatment on Drp1 protein levels were similar, supporting our hypothesis that H$_2$S hindered mitochondrial fission by reducing Drp1 expression. However, the effects of H$_2$S on other signaling pathways, including the phosphoinositide 3-kinase/AKT serine-threonine kinase and c-Jun N-terminal kinase pathways, require further investigation.

In conclusion, the results of the present study support the hypothesis that H$_2$S may downregulate Drp1 expression and inhibit mitochondrial fission, and that these effects may involve the ERK1/2 signaling pathway. These results lay a foundation for an improved understanding of the effects of the novel gaseous signaling molecule H$_2$S on mitochondrial function. However, further studies *in vivo* are required to confirm this hypothesis.

Acknowledgements

References

1. Lin MT and Beal MF: Mitochondrial dysfunction and oxidative stress in neurodegenerative diseases. Nature 443: 787-795, 2006.
2. Westermann B: Mitochondrial fusion and fission in cell life and death. Nat Rev Mol Cell Biol 11: 872-884, 2010.
3. Chen H, Chomyn A and Chan DC: Disruption of fusion results in mitochondrial heterogeneity and dysfunction. J Biol Chem 280: 26185-26192, 2005.
4. Chen H, Vermulst M, Wang YE, Chomyn A, Prolla TA, McCaffery JM and Chan DC: Mitochondrial fusion is required for mtDNA stability in skeletal muscle and tolerance of mtDNA mutations. Cell 141: 280-289, 2010.
5. Frank S, Gaume B, Bergmann-Leitner ES, Leitner WW, Robert EG, Catez F, Smith CL and Youle RJ: The role of dynamin-related protein 1, a mediator of mitochondrial fission, in apoptosis. Dev Cell 1: 515-525, 2001.
6. Gomes LC, Di Benedetto G and Scorrano L: During autophagy mitochondria elongate, are spared from degradation and sustain cell viability. Nat Cell Biol 13: 589-598, 2011.
7. Twig G, Elorza A, Molina AJ, Mohamed H, Wikstrom JD, Walzer G, Stiles L, Haigh SE, Katz S, Las G, et al: Fission and selective fusion govern mitochondrial segregation and elimination by autophagy. EMBO J 27: 433-446, 2008.
8. Karbowski M: Mitochondria on guard: Role of mitochondrial fusion and fission in the regulation of apoptosis. Adv Exp Med Biol 687: 131-142, 2010.
9. Qi X, Qvit N, Su YC and Mochly-Rosen D: A novel Drp1 inhibitor diminishes aberrant mitochondrial fission and neurotoxicity. J Cell Sci 126: 789-802, 2013.
10. Xie N, Wang C, Lian Y, Wu C, Zhang H and Zhang Q: Inhibition of mitochondrial fission attenuates Aβ-induced microglia apoptosis. Neuroscience 256: 36-42, 2014.
11. Chen H, McCaffery JM and Chan DC: Mitochondrial fusion protects against neurodegeneration in the Cerebellum. Cell 130: 548-562, 2007.
12. Baloyannis SJ: Mitochondrial alterations in Alzheimer's disease. J Alzheimers Dis 9: 119-126, 2006.
13. Bossy-Wetzel E, Barsoum MJ, Godzik A, Schwarzenbacher R and Lipton SA: Mitochondrial fission in apoptosis, neurodegeneration and aging. Curr Opin Cell Biol 15: 706-716, 2003.
14. Bonda DJ, Wang X, Perry G, Smith MA and Zhu X: Mitochondrial dynamics in Alzheimer's disease: Opportunities for future treatment strategies. Drugs Aging 27: 181-192, 2010.
15. Su B, Wang X, Bonda D, Perry G, Smith M and Zhu X: Abnormal mitochondrial dynamics-a novel therapeutic target for Alzheimer's disease? Mol Neurobiol 41: 87-96, 2010.
16. Whiteman M, Le Trionnaire S, Chopra M, Fox B and Whatmore J: Emerging role of hydrogen sulfide in health and disease: Critical appraisal of biomarkers and pharmacological tools. Clin Sci (Lond) 121: 459-488, 2011.
17. Fiorucci S, Distrutti E, Cirino G and Wallace JL: The emerging roles of hydrogen sulfide in the gastrointestinal tract and liver. Gastroenterology 131: 259-271, 2006.
18. Shibuya N, Tanaka M, Yoshida M, Ogasawara Y, Togawa T, Ishii K and Kimura H: 3-Mercaptopyr-uvate sulfurtransferase produces hydrogen sulfide and bound sulfane sulfur in the brain. Antioxid Redox Signal 11: 703-714, 2009.
19. Kimura Y, Goto Y and Kimura H: Hydrogen sulfide increases glutathione production and suppresses oxidative stress in mitochondria. Antioxid Redox Signal 12: 1-13, 2010.
20. Whiteman M, Armstrong JS, Chu SH, Jia-Ling S, Wong BS, Cheung NS, Halliwell B and Moore PK: The novel neuromodulator hydrogen sulfide: An endogenous peroxynitrite 'scavenger'? J Neurochem 90: 765-768, 2004.
21. Mikami Y, Shibuya N, Kimura Y, Nagahara N, Yamada M and Kimura H: Hydrogen sulfide protects the retina from light-induced degeneration by the modulation of Ca2+ influx. J Biol Chem 286: 39379-39386, 2011.
22. Elrod JW, Calvert JW, Morrison J, Doeller JE, Kraus DW, Tao L, Jiao X, Scalia R, Kiss L, Szabo C, et al: Hydrogen sulfide attenuates myocardial ischemia-reperfusion injury by preservation of mitochondrial function. Proc Natl Acad Sci USA 104: 15560-15565, 2007.
23. Szabo C, Ransy C, Módis K, Andriamihaja M, Murghes B, Coletta C, Olah G, Yanagi K and Bouillaud F: Regulation of mitochondrial bioenergetic function by hydrogen sulfide. Part I. Biochemical and physiological mechanisms. Br J Pharmacol 171: 2099-2122, 2014.
24. Reddy PH: Inhibitors of mitochondrial fission as a therapeutic strategy for diseases with oxidative stress and mitochondrial dysfunction. J Alzheimers Dis 40: 245-256, 2014.
25. Calkins MJ, Manczak M, Mao P, Shirendeb U and Reddy PH: Impaired mitochondrial biogenesis, defective axonal transport of mitochondria, abnormal mitochondrial dynamics and synaptic degeneration in a mouse model of Alzheimer's disease. Hum Mol Genet 20: 4515-4529, 2011.
26. Du H, Guo L, Yan S, Sosunov AA, McKhann GM and Yan SS: Early deficits in synaptic mitochondria in an Alzheimer's disease mouse model. Proc Natl Acad Sci USA 107: 18670-18675, 2010.
27. Livak KJ and Schmittgen TD: Analysis of relative gene expression data using real-time quantitative PCR and the 2(-Delta Delta C(T)) Method. Methods 25: 402-408, 2001.
28. Abe K and Kimura H: The possible role of hydrogen sulfide as an endogenous neuromodulator. J Neurosci 16: 1066-1071, 1996.
29. Zanardo RC, Brancaleone V, Distrutti E, Fiorucci S, Cirino G and Wallace JL: Hydrogen sulfide is an endogenous modulator of leukocyte-mediated inflammation. FASEB J 20: 2118-2120, 2006.
30. Kaneko Y, Kimura Y, Kimura H and Niki I: L-cysteine inhibits insulin release from the pancreatic beta-cell: Possible involvement of metabolic production of hydrogen sulfide, a novel gasotransmitter. Diabetes 55: 1391-1397, 2006.
31. Nisoli E, Falcone S, Tonello C, Cozzi V, Palomba L, Fiorani M, Pisconti A, Brunelli S, Cardile A, Francolini M, et al: Mitochondrial biogenesis by NO yields functionally active mitochondria in mammals. Proc Natl Acad Sci USA 101: 16507-16512, 2004.
32. Shen Y, Guo W, Wang Z, Zhang Y, Zhong L and Zhu Y: Protective effects of hydrogen sulfide in hypoxic human umbilical vein endothelial cells: A possible mitochondria-dependent pathway. Int J Mol Sci 14: 13093-13108, 2013.
33. Wen YD, Wang H, Kho SH, Rinkiko S, Sheng X, Shen HM and Zhu YZ: Hydrogen sulfide protects HUVECs against hydrogen peroxide induced mitochondrial dysfunction and oxidative stress. PLoS One 8: e53147, 2013.
34. Barsoum MJ, Yuan H, Gerencser AA, Liot G, Kushnareva Y, Gräber S, Kovacs I, Lee WD, Waggoner J, Cui J, et al: Nitric oxide-induced mitochondrial fission is regulated by dynamin-related GTPases in neurons. EMBO J 25: 3900-3911, 2006.
35. Zhang H, Gao Y, Zhao F, Dai Z, Meng T, Tu S and Yan Y: Hydrogen sulfide reduces mRNA and protein levels of β-site amyloid precursor protein cleaving enzyme 1 in PC12 cells. Neurochem Int 58: 169-175, 2011.
36. Gan X, Huang S, Wu L, Wang Y, Hu G, Li G, Zhang H, Yu H, Swerdlow RH, Chen JX and Yan SS: Inhibition of ERK-DLP1 signaling and mitochondrial division alleviates mitochondrial dysfunction in Alzheimer's disease cybrid cell. Biochim Biophys Acta 1842: 220-231, 2014.